EURASIP Journal on Applied Signal Processing 2004:13, 1993–2001


# Non-Data-Aided Feedforward Carrier Frequency Offset Estimators for QAM Constellations: A Nonlinear Least-Squares Approach

**Y. Wang**
*Department of Electrical Engineering, Texas A&M University, College Station, TX 77843-3128, USA*
*Email: wangyan@ee.tamu.edu*

**K. Shi**
*Department of Electrical Engineering, Texas A&M University, College Station, TX 77843-3128, USA*
*Email: kaishi@ee.tamu.edu*

**E. Serpedin**
*Department of Electrical Engineering, Texas A&M University, College Station, TX 77843-3128, USA*
*Email: serpedin@ee.tamu.edu*

*Received 21 February 2003; Revised 17 March 2004; Recommended for Publication by Tomohiko Taniguchi*

This paper performs a comprehensive performance analysis of a family of non-data-aided feedforward carrier frequency offset estimators for QAM signals transmitted through AWGN channels in the presence of unknown timing error. The proposed carrier frequency offset estimators are asymptotically (large sample) nonlinear least-squares estimators obtained by exploiting the fourth-order conjugate cyclostationary statistics of the received signal and exhibit fast convergence rates (asymptotic variances on the order of $O(N^{-3})$, where $N$ stands for the number of samples). The exact asymptotic performance of these estimators is established and analyzed as a function of the received signal sampling frequency, signal-to-noise ratio, timing delay, and number of symbols. It is shown that in the presence of intersymbol interference effects, the performance of the frequency offset estimators can be improved significantly by oversampling (or fractionally sampling) the received signal. Finally, simulation results are presented to corroborate the theoretical performance analysis, and comparisons with the modified Cramér-Rao bound illustrate the superior performance of the proposed nonlinear least-squares carrier frequency offset estimators.

**Keywords and phrases:** synchronization, cyclostationary, non-data-aided estimation, harmonic retrieval, carrier frequency offset.

## 1. INTRODUCTION

In mobile wireless communication channels, loss of synchronization may occur due to carrier frequency offset (FO) and/or Doppler effects. Non-data-aided (or blind) feedforward carrier FO estimation schemes present high potential for synchronization of burst-mode transmissions and spectrally efficient modulations because they do not require long acquisition intervals and bandwidth consuming training sequences. For these reasons, non-data-aided carrier compensation schemes have found applications in synchronization of broadcast networks and can be used in many practical receivers where a coarse carrier FO correction is applied in front of the matched filter.

Non-data-aided feedforward carrier FO estimators have been proposed and analyzed in various contexts by many researchers [1, 2, 3, 4, 5, 6, 7, 8]. The common feature of these algorithms relies on the cyclostationary (CS) statistics of the received waveform that have been extensively exploited in communication systems to perform tasks of synchronization, blind channel identification, and equalization (see, e.g., [1, 2, 3, 4, 5, 6, 7, 8, 9, 10, 11, 12]), and are induced either by oversampling of the received analog waveform [5, 7, 8], or by filtering the received discrete-time sequence through a nonlinear filter [1, 3]. This latter category of estimators exploits the second and/or the higher-order CS statistics of the received sequence, exhibits high convergence rates (asymptotic variance on the order of $O(N^{-3})$, where $N$ stands for the number of samples), and the estimators can be interpreted as nonlinear least-squares (NLS) estimators.

This paper proposes to study the exact asymptotic (large sample) performance of a family of NLS carrier FO

estimators for QAM transmissions in the presence of channel intersymbol interference (ISI) effects and to suggest new algorithms with improved performance. The exact asymptotic variance of this family of estimators is established in closed-form expression and it is shown that these estimators exhibit high convergence rates close to the modified Cramér-Rao bound (CRB).

The rest of this paper is organized as follows. In Section 2, the discrete-time channel model is established and the necessary modeling assumptions are invoked. Section 3 describes a class of non-data-aided feedforward carrier FO estimators, and Section 4 briefly illustrates the equivalence between these FO estimators and the NLS spectrum estimators. Based on this equivalence, the asymptotic performance analysis of the proposed FO estimators is established in closed-form expression. In Section 5, simulation results are conducted to confirm our theoretical analysis. Finally, in Section 6, conclusions and possible extensions of the proposed work are discussed. Detailed mathematical derivations for the performance analysis of the proposed FO estimators are reported in appendices http://ee.tamu.edu/~serpedin.

## 2. MODELING ASSUMPTIONS

Supposing that a QAM signal is transmitted through an AWGN channel, the complex envelope of the received signal is affected by the carrier FO and/or Doppler shift $F_e$ and is expressed as[1] (see [7] and [13, Chapter 14])

$$r_c(t) = e^{j(2\pi F_e t+\theta)} \sum_l w(l) h_c^{(\mathrm{tr})}(t - lT - \epsilon T) + v_c(t), \qquad (1)$$

where $w(l)$'s are the transmitted complex information symbols, $h_c^{(\mathrm{tr})}(t)$ denotes the transmitter's signaling pulse, $v_c(t)$ is the complex-valued additive noise assumed independently distributed with respect to the input symbol sequence $w(n)$, $T$ is the symbol period, and $\epsilon$ is an unknown normalized timing error introduced by the channel. Since the unknown carrier phase offset $\theta$ does not play any role in the ensuing derivations, it will be omitted ($\theta = 0$). After matched filtering with $h_c^{(\mathrm{rec})}(t)$, the resulting signal is (over-)sampled at a period $T_s := T/P$, where the oversampling factor $P \geq 1$ is an integer. It is well known that more general antialiasing receive filters are possible, but the analysis does not support any significant change. Under the common assumption that the FO achieves small values ($F_e T < 0.1$), the following equivalent discrete-time model can be deduced:

$$x(n) = e^{j2\pi f_e n} \sum_l w(l) h(n - lP) + v(n), \qquad (2)$$

where $f_e := F_e T_s$, $x(n) := (r_c(t) * h_c^{(\mathrm{rec})}(t))|_{t=nT_s}$ ($*$ denotes convolution), $v(n) := (v_c(t) * h_c^{(\mathrm{rec})}(t))|_{t=nT_s}$, and $h(n) := (h_c^{(\mathrm{tr})}(t) * h_c^{(\mathrm{rec})}(t))|_{t=nT_s-\epsilon T}$. For large FO ($F_e T \geq 0.1$), a very similar model to (2) results. Indeed, from (1), the receiver output after sampling can be expressed as

$$\begin{aligned} x(n) &:= (r_c(t) * h_c^{(\mathrm{rec})}(t))|_{t=nT_s} \\ &= \sum_l w(l) \int h_c^{(\mathrm{rec})}(\tau) h_c^{(\mathrm{tr})}(nT_s - \tau - lT - \epsilon T) \\ &\qquad \times e^{j2\pi F_e (nT_s-\tau)} d\tau + v(nT_s) \\ &= e^{j2\pi F_e nT_s} \sum_l w(l) \int h_c^{(\mathrm{rec})}(\tau) h_c^{(\mathrm{tr})}(nT_s - \tau - lT - \epsilon T) \\ &\qquad \times e^{-j2\pi F_e \tau} d\tau + v(nT_s) \\ &= e^{j2\pi f_e n} \sum_l w(l) h'(n - lP) + v(n), \end{aligned} \qquad (3)$$

where $h'(n) := h_c'(t)|_{t=nT_s-\epsilon T}$ and $h_c'(t) = h_c^{(\mathrm{tr})}(t) * h_c^{(\mathrm{rec})}(t) \exp(-j2\pi F_e t)$. Substituting $h(n)$ with $h'(n)$, we observe the equivalence between the two models (2) and (3), corresponding to small and large carrier FOs, respectively. Because estimation of large and small FOs can be achieved using the same estimation framework, we restrict our analysis in what follows to the problem of estimating small carrier FOs assuming the channel model (2). Moreover, since no knowledge of the timing delay is assumed, the proposed FO estimators will apply also to general frequency-selective channels.

In order to derive the asymptotic performance of the FO estimators without any loss of generality, the following assumptions are imposed.

(AS1) $w(n)$ is a zero-mean independently and identically distributed (i.i.d.) sequence with values drawn from a QAM constellation with unit variance, that is, $\sigma_{2w}^2 := \mathrm{E}\{|w(n)|^2\} = 1$.

(AS2) $v_c(t)$ is white circularly distributed Gaussian noise with zero mean and variance $\sigma_{2v}^2$.

(AS3) $v(n)$ satisfies the so-called mixing condition [14, pages 8, 25–27], which states that the $k$th-order cumulant[2] of $v(n)$ at lag $\boldsymbol{\tau} := (\tau_1, \tau_2, \ldots, \tau_{k-1})$, denoted by $c_{kv}(\boldsymbol{\tau}) := \mathrm{cum}\{v(n), v(n+\tau_1), \ldots, v(n+\tau_{k-1})\}$, is absolutely summable: $\sum_{\boldsymbol{\tau}} |c_{kv}(\boldsymbol{\tau})| < \infty$, for all $k$. The mixing condition is a reasonable assumption in practice since it is satisfied by all signals with finite memory. Assumption (AS3) will prove useful in facilitating calculation of the asymptotic performance of the proposed estimators. Also, the following definition of cumulant will be used extensively: if $x_1, \ldots, x_p$ are $p$ random variables,

[1] The subscript $c$ is used to denote a continuous-time signal.

[2] For a detailed presentation of the concept of cumulant, please refer to [14, pages 19–21] and [15].

the $p$th-order joint cumulant of $x_1, \ldots, x_p$ is defined as

$$\begin{aligned}&\operatorname{cum}(x_1, \ldots, x_p)\\ &:= \sum (-1)^{k-1}(k-1)!\left(E\prod_{j\in\mu_1} x_j\right)\cdots\left(E\prod_{j\in\mu_k} x_j\right),\end{aligned} \tag{4}$$

where the summation operator assumes all the partitions $(\mu_1, \ldots, \mu_k)$, $k = 1, \ldots, p$, of $(1, \ldots, p)$.

## 3. CARRIER FREQUENCY OFFSET ESTIMATORS

Estimating $f_e$ from $x(n)$ in (2) amounts to retrieving a complex exponential embedded in multiplicative noise $\sum_l w(l)h(n-lP)$ and additive noise $v(n)$. The underlying idea for estimating the FO is to interpret the higher-order statistics of the received signal as a sum of several constant amplitude harmonics embedded in (CS) noise, and to extract the FO from the frequencies of these spectral lines. We will solve this spectral estimation problem by interpreting it from a CS-statistics viewpoint. Due to their $\pi/2$-rotationally invariant symmetry properties, all QAM constellations satisfy the moment conditions $\mathrm{E}\{w^2(n)\} = \mathrm{E}\{w^3(n)\} = 0$, $\mathrm{E}\{w^4(n)\} \neq 0$. This property will be exploited next to design FO estimators based on the fourth-order CS-statistics of the received sequence.

Define the fourth-order conjugate time-varying correlations (for QAM constellations, the fourth-order cumulants and moments coincide) of the received sequence $x(n)$ via $\tilde{c}_{4x}(n;\mathbf{0}) := \mathrm{E}\{x^4(n)\}$, with $\mathbf{0} := [0 \;\; 0 \;\; 0]$. For $P = 1$, it turns out that

$$\tilde{c}_{4x}(n;\mathbf{0}) = \tilde{\kappa}_4 e^{j2\pi 4 f_e n}\sum_l h^4(l), \tag{5}$$

with $\tilde{\kappa}_4 := \operatorname{cum}\{w(n), w(n), w(n), w(n)\} = \mathrm{E}\{w^4(n)\}$. Similarly, for $P > 1$, it follows that

$$\tilde{c}_{4x}(n;\mathbf{0}) = \tilde{\kappa}_4 e^{j2\pi 4 f_e n}\sum_l h^4(n-lP). \tag{6}$$

Being almost periodic with respect to $n$, the generalized Fourier Series (FS) coefficient of $\tilde{c}_{4x}(n;\mathbf{0})$, termed the conjugate cyclic correlation, can be expressed for $P = 1$ as (cf. [16])

$$\begin{aligned}\widetilde{C}_{4x}(\alpha;\mathbf{0}) &:= \lim_{N\to\infty}\frac{1}{N}\sum_{n=0}^{N-1}\tilde{c}_{4x}(n;\mathbf{0})e^{-j2\pi\alpha n}\\ &= \widetilde{C}_{4x}(\alpha_0;\mathbf{0})\delta(\alpha-\alpha_0),\end{aligned} \tag{7}$$

where $\widetilde{C}_{4x}(\alpha_0;\mathbf{0}) = \tilde{\kappa}_4\sum_l h^4(l)$ and $\alpha_0 := 4f_e$. When $P > 1$, it follows that

$$\widetilde{C}_{4x}(\alpha;\mathbf{0}) = \sum_{k=0}^{P-1}\widetilde{C}_{4x}\left(\alpha_0+\frac{k}{P};\mathbf{0}\right)\delta\left(\alpha-\left(\alpha_0+\frac{k}{P}\right)\right), \tag{8}$$

where $\widetilde{C}_{4x}(\alpha_0 + k/P;\mathbf{0}) = (\tilde{\kappa}_4/P)\sum_n h^4(n)\exp(-j2\pi kn/P)$.

Thus, $\widetilde{C}_{4x}(\alpha;\mathbf{0})$ consists of a single spectral line located at $4f_e$ when $P = 1$, and $P$ spectral lines located at the cyclic frequencies $4f_e + k/P$, $k = 0, 1, \ldots, P-1$, when $P > 1$. An estimator of $f_e$ can be obtained by determining the location of the spectral line present in $\widetilde{C}_{4x}(\alpha;\mathbf{0})$ (see (7)):

$$f_e = \frac{1}{4}\left(\arg\max_{\dot{\alpha}\in(-0.5,0.5)}\left|\widetilde{C}_{4x}(\dot{\alpha};\mathbf{0})\right|^2\right), \tag{9}$$

where the variable with a dot denotes a trial value. In practice, a computationally efficient FFT-based implementation of (9) can be obtained by adopting an asymptotically consistent sample estimator for the conjugate cyclic correlation $\widetilde{C}_{4x}(\alpha;\mathbf{0})$, which takes the following form:

$$\hat{\widetilde{C}}_{4x}(\alpha;\mathbf{0}) := \frac{1}{N}\sum_{n=0}^{N-1}x^4(n)e^{-j2\pi\alpha n}. \tag{10}$$

Plugging (10) back into (9), we obtain the estimator

$$\begin{aligned}\hat{f}_e &= \frac{1}{4}\left(\arg\max_{\dot{\alpha}\in(-0.5,0.5)}\left|\hat{\widetilde{C}}_{4x}(\dot{\alpha};\mathbf{0})\right|^2\right)\\ &= \frac{1}{4}\left(\arg\max_{\dot{\alpha}\in(-0.5,0.5)}\left|\frac{1}{N}\sum_{n=0}^{N-1}x^4(n)e^{-j2\pi\dot{\alpha}n}\right|^2\right).\end{aligned} \tag{11}$$

In the case when $P > 1$, it is possible to design an FO estimator that extracts $f_e$ solely from knowledge of the location information of the spectral line of largest magnitude ($k = 0$). However, this approach leads again to the estimator (11). A different alternative is to extract the FO by exploiting jointly the location information of all the $P$ spectral lines. In this case, the FFT-based FO estimator is obtained as follows:

$$\begin{aligned}\hat{\alpha}_N &:= 4\hat{f}_e = \arg\max_{|\dot{\alpha}|<1/(2P)} J_N(\dot{\alpha}),\\ J_N(\dot{\alpha}) &:= \sum_{k=0}^{P-1}\left|\hat{\widetilde{C}}_{4x}\left(\dot{\alpha}+\frac{k}{P};\mathbf{0}\right)\right|^2\\ &= \sum_{k=0}^{P-1}\left|\frac{1}{N}\sum_{n=0}^{N-1}x^4(n)e^{-j2\pi(\dot{\alpha}+k/P)n}\right|^2.\end{aligned} \tag{12}$$

Note that the condition $|F_e T| \leq 1/8$ is required in (11) and (12) in order to ensure identifiability of $F_e T$.

In the next section, we will establish, in a unified manner, the asymptotic performance of the proposed frequency estimators (11) and (12), and show the interrelation between the present class of cyclic estimators and the family of NLS estimators.

## 4. ASYMPTOTIC PERFORMANCE ANALYSIS

In order to show the equivalence between the present carrier FO estimation problem and the problem of estimating the frequencies of a number of harmonics embedded in noise, it is helpful to observe that the conjugate time-varying

correlation $\tilde{c}_{4x}(n;\mathbf{0})$ can be expressed as

$$\begin{aligned}\tilde{c}_{4x}(n;\mathbf{0}) &= \sum_{k=0}^{P-1} \widetilde{C}_{4x}\left(\alpha_0+\frac{k}{P};\mathbf{0}\right)e^{j2\pi(\alpha_0+k/P)n}\\ &= \sum_{k=0}^{P-1}\lambda_k e^{j(\omega_k n+\phi_k)},\end{aligned} \tag{13}$$

where $\lambda_k \exp(j\phi_k) := \widetilde{C}_{4x}(\alpha_0 + k/P;\mathbf{0})$ and $\omega_k := (2\pi k/P) + 2\pi\alpha_0$.

Defining the zero-mean stochastic process $e(n)$ as

$$\begin{aligned}e(n) &:= x^4(n) - \mathrm{E}\{x^4(n)\}\\ &= x^4(n) - \sum_{k=0}^{P-1}\widetilde{C}_{4x}\left(\alpha_0+\frac{k}{P};\mathbf{0}\right)e^{j2\pi(k/P+\alpha_0)n},\end{aligned} \tag{14}$$

it follows that

$$\begin{aligned}x^4(n) &= \sum_{k=0}^{P-1}\widetilde{C}_{4x}\left(\alpha_0+\frac{k}{P};\mathbf{0}\right)e^{j2\pi(k/P+\alpha_0)n} + e(n)\\ &= \sum_{k=0}^{P-1}\lambda_k e^{j(\omega_k n+\phi_k)} + e(n).\end{aligned} \tag{15}$$

Thus, $x^4(n)$ can be interpreted as the sum of $P$ constant amplitude harmonics corrupted by the CS noise $e(n)$ [3].

Consider the NLS estimator

$$\hat{\boldsymbol{\theta}} := \arg\min_{\dot{\boldsymbol{\theta}}} J(\dot{\boldsymbol{\theta}}), \tag{16}$$

$$J(\dot{\boldsymbol{\theta}}) := \frac{1}{2N}\sum_{n=0}^{N-1}\left|x^4(n) - \sum_{k=0}^{P-1}\dot{\lambda}_k e^{j\dot{\phi}_k}e^{j2\pi(\dot{\alpha}+k/P)n}\right|^2, \tag{17}$$

with the vector $\dot{\boldsymbol{\theta}} := [\dot{\lambda}_0 \ \cdots \ \dot{\lambda}_{P-1} \ \dot{\phi}_0 \ \cdots \ \dot{\phi}_{P-1} \ \dot{\alpha}]^{\mathrm{T}}$, superscript T standing for transposition. It can be shown that the FFT-based estimator (12) is asymptotically equivalent to the NLS estimator (16) (see, e.g., [3, 9]). Hence, the proposed cyclic FO estimator can be viewed as the NLS estimator and the estimate $\hat{\alpha}_N$ is asymptotically unbiased and consistent [17, 18]. In order to compute the asymptotic performance of estimator (12), it suffices to establish the asymptotic performance of NLS estimator (16). The following result, whose proof is deferred to Appendix 1 at http://ee.tamu.edu/~serpedin for space limitation reasons, holds.[3]

Theorem 1. *The asymptotic variance of the estimate $\hat{\alpha}_N$ is given by*

$$\gamma := \lim_{N\to\infty} N^3\,\mathrm{E}\left\{\left(\hat{\alpha}_N-\alpha_0\right)^2\right\} = \frac{3\sum_{l_1,l_2=0}^{P-1}\mathbf{R}_{l_1}^{\mathrm{H}}\mathbf{G}_{l_1,l_2}\mathbf{R}_{l_2}}{\pi^2\left(\sum_{l=0}^{P-1}\mathbf{R}_l^{\mathrm{H}}\mathbf{R}_l\right)^2}, \tag{18}$$

*with*

$$\mathbf{R}_l := \begin{bmatrix}\widetilde{C}_{4x}\left(\alpha_0+\dfrac{l}{P};\mathbf{0}\right)\\ \widetilde{C}^*_{4x}\left(\alpha_0+\dfrac{l}{P};\mathbf{0}\right)\end{bmatrix},$$

$$\mathbf{G}_{l_1,l_2} := \begin{bmatrix} S_{2e}\left(\dfrac{l_1-l_2}{P};\alpha_0+\dfrac{l_1}{P}\right) & -\widetilde{S}_{2e}\left(2\alpha_0+\dfrac{l_1+l_2}{P};\alpha_0+\dfrac{l_1}{P}\right)\\ -\widetilde{S}^*_{2e}\left(2\alpha_0+\dfrac{l_1+l_2}{P};\alpha_0+\dfrac{l_1}{P}\right) & S^*_{2e}\left(\dfrac{l_1-l_2}{P};\alpha_0+\dfrac{l_1}{P}\right)\end{bmatrix}, \tag{19}$$

*and $S_{2e}(\alpha;f)$ and $\widetilde{S}_{2e}(\alpha;f)$ stand for the unconjugate and conjugate cyclic spectra of $e(n)$ at cycle $\alpha$ and frequency $f$, defined as*

$$\begin{aligned}S_{2e}(\alpha;f) &:= \sum_{\tau}\lim_{N\to\infty}\frac{1}{N}\sum_{n=0}^{N-1}\mathrm{E}\{e^*(n)e(n+\tau)\}e^{-j2\pi\alpha n}e^{-j2\pi f\tau},\\ \widetilde{S}_{2e}(\alpha;f) &:= \sum_{\tau}\lim_{N\to\infty}\frac{1}{N}\sum_{n=0}^{N-1}\mathrm{E}\{e(n)e(n+\tau)\}e^{-j2\pi\alpha n}e^{-j2\pi f\tau},\end{aligned} \tag{20}$$

*respectively.*

As an immediate corollary of Theorem 1, in the case when only the spectral line with the largest magnitude is considered, we obtain that the asymptotic variance of estimator (11) is given by

$$\lim_{N\to\infty} N^3\,\mathrm{E}\left\{\left(\hat{\alpha}_N-\alpha_0\right)^2\right\} = \frac{3\mathbf{R}_0^{\mathrm{H}}\mathbf{G}_{0,0}\mathbf{R}_0}{\pi^2\left\|\mathbf{R}_0\right\|^4}. \tag{21}$$

Note that when $P = 1$, the autocorrelation $c_{2e}(n;\tau) := \mathrm{E}\{e^*(n)e(n+\tau)\}$ depends only on the lag $\tau$, hence $e(n)$ is stationary with respect to its second-order autocorrelation function and the cyclic spectrum $S_{2e}(0;\alpha_0)$ coincides with the second-order stationary spectrum $S_{2e}(\alpha_0)$. Result (21) shows that the asymptotic variance of $\widehat{F_e T}$ converges as $O(N^{-3})$ and depends inversely proportionally on the signal-to-noise ratio (SNR) corresponding to the $k = 0$ spectral line[4] $\mathrm{SNR}_0 := |\widetilde{C}_{4x}(\alpha_0;\mathbf{0})|^2/\,\mathrm{re}\{S_{2e}(0;\alpha_0) - \widetilde{S}_{2e}(2\alpha_0;\alpha_0)\}$.

Evaluation of asymptotic variance (18) requires calculation of the unconjugate/conjugate cyclic spectra, $S_{2e}(\alpha;f)$ and $\widetilde{S}_{2e}(\alpha;f)$, whose closed-form expressions will be sketched in what follows.

Define the variables

$$\begin{aligned}\kappa_8 &:= \mathrm{cum}\{\underbrace{w^*(n),\ldots,w^*(n)}_{4},\underbrace{w(n),\ldots,w(n)}_{4}\},\\ \tilde{\kappa}_8 &:= \mathrm{cum}\{\underbrace{w(n),\ldots,w(n)}_{8}\},\end{aligned} \tag{22}$$

[3] The superscripts $*$ and H stand for conjugation and conjugate transposition, respectively.

[4] The notations "re" and "im" stand for the real and imaginary parts, respectively.

and define the fourth- and sixth-order ($l = 4, 6$) moments/cyclic moments of $x(n)$ as follows:

$$\begin{aligned} m_{lx}(n;\underbrace{0,\ldots,0}_{l/2-1},\underbrace{\tau,\ldots,\tau}_{l/2}) &:= \mathrm{E}\{x^{*l/2}(n)x^{l/2}(n+\tau)\}, \\ M_{lx}(k;\underbrace{0,\ldots,0}_{l/2-1},\underbrace{\tau,\ldots,\tau}_{l/2}) &:= \frac{1}{P}\sum_{n=0}^{P-1} m_{lx}(n;\underbrace{0,\ldots,0}_{l/2-1},\underbrace{\tau,\ldots,\tau}_{l/2})e^{-j2\pi kn/P}. \end{aligned} \tag{23}$$

Some lengthy calculations, the details of which are illustrated in Appendix 2 at http://ee.tamu.edu/~serpedin, show that the following results hold.

Proposition 1. *For $P = 1$, the unconjugate/conjugate cyclic spectra of $e(n)$ are given by*

$$\begin{aligned} &S_{2e}(\alpha_0) \\ &= \sum_{\tau}\big[16m_{2x}(\tau)m_{6x}(0,0,\tau,\tau,\tau) + 18m_{4x}^2(0,\tau,\tau) \\ &\qquad - 144m_{2x}^2(\tau)m_{4x}(0,\tau,\tau) + 144m_{2x}^4(\tau)\big]e^{-j2\pi\alpha_0\tau} \\ &\quad + \frac{\kappa_8}{\widetilde{\kappa}_4^2}\,|\,\widetilde{C}_{4x}(\alpha_0;\mathbf{0})\,|^2, \\ &\widetilde{S}_{2e}(2\alpha_0;\alpha_0) \\ &= \sum_{\tau}\Bigg[\tilde{\kappa}_8\sum_l h^4(l)h^4(l+\tau) \\ &\qquad + 16\tilde{\kappa}_4^2\sum_l h(l)h^3(l+\tau)\cdot\sum_l h^3(l)h(l+\tau) \\ &\qquad + 18\tilde{\kappa}_4^2\Big(\sum_l h^2(l)h^2(l+\tau)\Big)^2\Bigg], \end{aligned} \tag{24}$$

*respectively.*

Proposition 2. *For $P > 1$, the unconjugate/conjugate cyclic spectra of $e(n)$ are given by*

$$\begin{aligned} &S_{2e}\Big(\frac{k}{P};\alpha_0+\frac{l}{P}\Big) \\ &= \sum_{\tau}\big[16\mathcal{V}_1 + 18\mathcal{V}_2 - 144\mathcal{V}_3 + 144\mathcal{V}_4\big]e^{-j2\pi(\alpha_0+l/P)\tau} \\ &\quad + \frac{\kappa_8 P}{\widetilde{\kappa}_4^2}\widetilde{C}_{4x}\Big(\alpha_0+\frac{l}{P};\mathbf{0}\Big)\widetilde{C}_{4x}^*\Big(\alpha_0+\frac{l-k}{P};\mathbf{0}\Big), \\ &\widetilde{S}_{2e}\Big(2\alpha_0+\frac{k}{P};\alpha_0+\frac{l}{P}\Big) \\ &= \sum_{\tau}\big[16\widetilde{\mathcal{V}}_1 + 18\widetilde{\mathcal{V}}_2 + \widetilde{C}_{8x}(k;\tau)\big]e^{-j2\pi l/P\tau}, \end{aligned} \tag{25}$$

*where*

$$\begin{aligned} \mathcal{V}_1 &:= \sum_{\substack{k_1,k_2=0\\ k_1+k_2-k\equiv 0 \bmod P}}^{P-1} M_{2x}(k_1;\tau)M_{6x}(k_2;0,0,\tau,\tau,\tau), \\ \mathcal{V}_2 &:= \sum_{\substack{k_1,k_2=0\\ k_1+k_2-k\equiv 0 \bmod P}}^{P-1} M_{4x}(k_1;0,\tau,\tau)M_{4x}(k_2;0,\tau,\tau), \\ \mathcal{V}_3 &:= \sum_{\substack{k_1,k_2,k_3=0\\ k_1+k_2+k_3-k\equiv 0 \bmod P}}^{P-1} M_{2x}(k_1;\tau)M_{2x}(k_2;\tau) \\ &\qquad \times M_{4x}(k_3;0,\tau,\tau), \\ \mathcal{V}_4 &:= \sum_{\substack{k_i=0\\ \sum_i k_i-k\equiv 0 \bmod P}}^{P-1} \prod_{i=0}^{3} M_{2x}(k_i;\tau), \\ \widetilde{\mathcal{V}}_1 &:= \sum_{\substack{k_1,k_2=0\\ k_1+k_2-k\equiv 0 \bmod P}}^{P-1} \widetilde{C}_{4x_1}(k_1;\tau)\widetilde{C}_{4x_3}(k_2;\tau), \\ \widetilde{\mathcal{V}}_2 &:= \sum_{\substack{k_1,k_2=0\\ k_1+k_2-k\equiv 0 \bmod P}}^{P-1} \widetilde{C}_{4x_2}(k_1;\tau)\widetilde{C}_{4x_2}(k_2;\tau), \\ \widetilde{C}_{4x_i}(k;\tau) &:= \frac{\widetilde{\kappa}_4}{P}\sum_n h^i(n)h^{(4-i)}(n+\tau)e^{-j2\pi(kn/P)}, \quad i = 1,2,3, \\ \widetilde{C}_{8x}(k;\tau) &:= \frac{\widetilde{\kappa}_8}{P}\sum_n h^4(n)h^4(n+\tau)e^{-j2\pi(kn/P)}. \end{aligned} \tag{26}$$

When $P = 1$, the discrete-time additive noise $v(n)$ is white. Then, it is not difficult to show that neither $S_{2e}(\alpha_0)$ nor $\widetilde{S}_{2e}(2\alpha_0;\alpha_0)$ depends on $f_e$. Therefore, the asymptotic variance (21) is independent of the unknown FO. The same conclusion can be obtained in the case of $P > 1$ if the SNR is large enough ($\sigma_{2v}^2 \ll 1$). However, it should be pointed out that when the channel model (3) applies, this independency generally does not hold.

To assess the performance of the proposed estimators, we derive the CRB as a benchmark, which is given as the inverse of the Fisher information matrix (FIM):

$$\mathbf{J}(f_e) = -\,\mathrm{E}\left\{\frac{\partial^2 \ln[\,\mathrm{E}_{\mathbf{w}}\{f_{\mathbf{X}}(\mathbf{x}\,|\,\mathbf{w};f_e)\}]}{\partial f_e^2}\right\}, \tag{27}$$

where $\mathbf{x} := [x(0)\ \ x(1)\ \ \cdots\ \ x(N-1)]^{\mathrm{T}}$ and $\mathbf{w}$ denotes the information symbol vector. Since the evaluation of exact CRB is computationally intractable, it is common to adopt a looser bound, the modified CRB (MCRB) [19], whose FIM is shown by direct calculations to take the following expression according to [20, Appendix 15C]:

$$\begin{aligned} \mathbf{J}(f_e) &= -\,\mathrm{E}_{\mathbf{w}}\,\mathrm{E}\left\{\frac{\partial^2 \ln[\,f_{\mathbf{X}}(\mathbf{x}\,|\,\mathbf{w};f_e)\,]}{\partial f_e^2}\right\} \\ &= 8\pi^2\,\mathrm{re}\left\{\sum_l \mathbf{h}_l^{\mathrm{H}}\mathbf{C}_v^{-1}\mathbf{h}_l\right\}, \end{aligned} \tag{28}$$

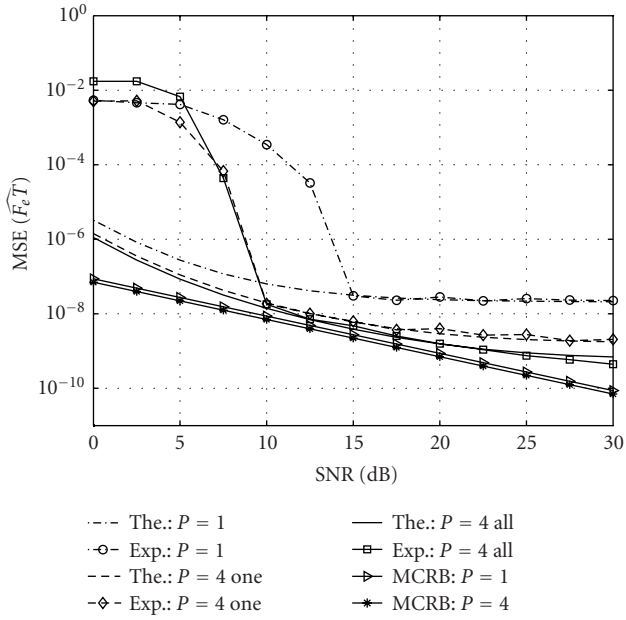


Figure 1: MSEs of $\widehat{F_eT}$ versus SNR.

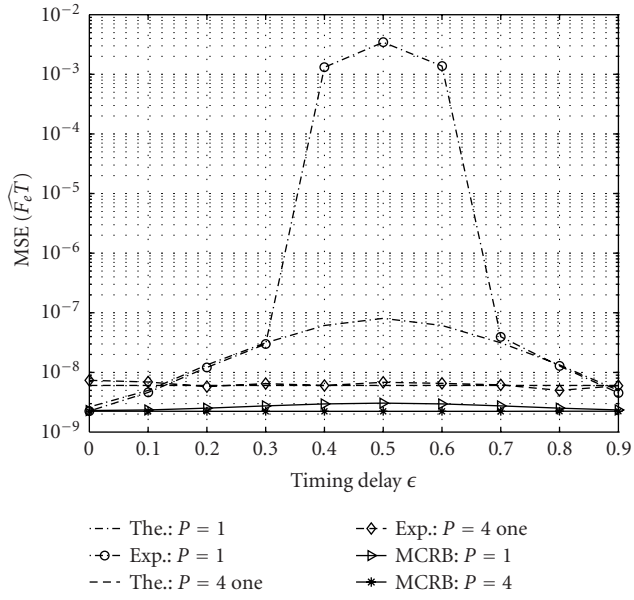


Figure 2: MSEs of $\widehat{F_eT}$ versus timing error $\epsilon$.

where

$$\mathbf{h}_l := \left[0 \; e^{j2\pi f_e} h(1-lP) \cdots (N-1)\, e^{j2(N-1)\pi f_e} h(N-1-lP)\right]^{\mathrm{T}}, \tag{29}$$

and the covariance matrix $\mathbf{C}_v$ of

$$\mathbf{v} := \begin{bmatrix} v(0) & v(1) & \cdots & v(N-1) \end{bmatrix}^{\mathrm{T}} \tag{30}$$

is a Toeplitz matrix of the following form:

$$\begin{aligned} \mathbf{C}_v &:= \mathrm{E}\left\{\mathbf{v}^{\mathrm{H}}\mathbf{v}\right\} = \sigma_{2v}^2 \mathbf{C}, \mathbf{C} \\ &:= \begin{bmatrix} h_d(0) & h_d(1) & \cdots & h_d(N-1) \\ h_d(1) & h_d(0) & \cdots & h_d(N-2) \\ \vdots & \ddots & \vdots & \vdots \\ h_d(N-1) & h_d(N-2) & \cdots & h_d(0) \end{bmatrix}, \end{aligned} \tag{31}$$

and $h_d(n) := (h_c^{(\mathrm{tr})}(t) * h_c^{(\mathrm{rec})}(t))|_{t=nT_s}$. Thus, we obtain

$$\mathrm{E}\left\{\left(\widehat{F}_e - F_e\right)^2\right\} \geq \frac{P^2}{T^2}\mathbf{J}^{-1}(f_e) = \frac{P^2\sigma_{2v}^2}{8\pi^2 T^2 \,\mathrm{re}\left\{\sum_l \mathbf{h}_l^{\mathrm{H}}\mathbf{C}^{-1}\mathbf{h}_l\right\}}. \tag{32}$$

Note that when $P = 1$, $\mathbf{C}$ is an identity matrix and

$$\begin{aligned} \mathrm{E}\left\{\left(\widehat{F}_e - F_e\right)^2\right\} &\geq \frac{\sigma_{2v}^2}{8\pi^2 T^2 \sum_l \sum_{n=0}^{N-1} n^2 \left|h(n-l)\right|^2} \\ &\doteq \frac{3\sigma_{2v}^2}{8\pi^2 T^2 N^3 \sum_{m=0}^{M} \left|h(m)\right|^2}, \end{aligned} \tag{33}$$

where $M$ is the order of channel $\{h(m)\}$, that is, the number of significant channel taps. It can be seen that in this case, the corresponding MCRB does not depend on the unknown FO.

## 5. SIMULATIONS

In this section, the experimental (Exp.) mean-square error (MSE) results and theoretical asymptotic bounds (The.) will be compared. The experimental results are obtained by performing 200 Monte Carlo trials. The transmitter and receiver filters are square-root raised cosine filters with roll-off factor $\rho = 0.5$ [13, Chapter 9], and the additive noise $v(n)$ is generated by passing Gaussian white noise through the square-root raised cosine filter to generate a sequence, with autocorrelation sequence $c_v(\tau) := E\{v^*(n)v(n+\tau)\} = \sigma_{2v}^2 h_{rc}(\tau)$, where $h_{rc}(t)$ stands for a raised cosine pulse [7]. The SNR is defined as $\mathrm{SNR} := 10\log_{10}(\sigma_{2w}^2/\sigma_{2v}^2)$. All the simulations are performed assuming the FO $F_eT = 0.011$ and, unless otherwise noted, the transmitted symbols are selected from a 4-QAM constellation, and the number of transmitted symbols is $L = 128$.

In all figures except Figures 3, 5, and 7, the theoretical bounds of estimators (11) and (12) for $P = 1$ and $P = 4$ are represented by the solid line, dash-dot line, and dash line, respectively. Their corresponding experimental results are plotted using the solid line with squares, dash-dot line with circles, and dash line with diamonds, respectively. The MCRB curves for $P = 1$ and $P = 4$ are shown as the solid lines with triangles and stars, respectively.

*Experiment* 1. *Performance with respect to SNR*

Assuming the timing error $\epsilon = 0.3$, in Figure 1 we compare the MSEs of FO estimators (11) and (12) with their theoretical asymptotic variances and MCRBs. It turns out that in the presence of ISI, the performance of FO estimator (11) can be significantly improved at medium and high SNRs by oversampling (fractionally sampling) the output signal. This result is further illustrated by Figure 2, where the MSE of FO estimator (11) is plotted versus timing error $\epsilon$, assuming again two different values for the oversampling

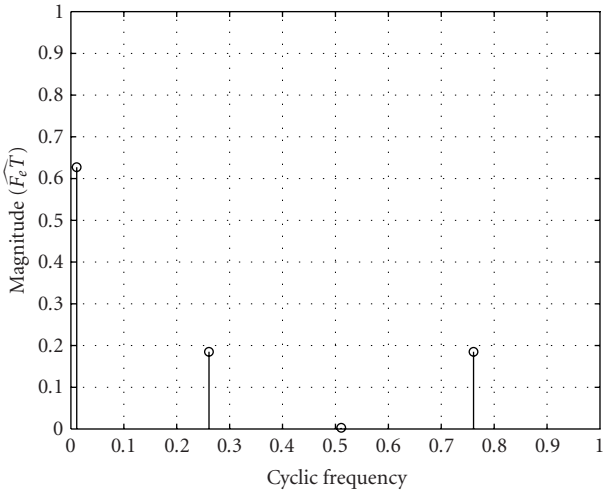


Figure 3: Amplitudes of harmonics with respect to cyclic frequency.

factors $P = 1$ and $P = 4$. An intuitive explanation that one can envisage for this result is to interpret the theoretical MSE expression of the carrier frequency estimator (see, e.g., (21)) as a ratio between a quantity that reflects the power of "self-noise" (the numerator of (21)) and the amplitude of the spectral line (the denominator of (21)). It is well known that oversampling induces CS statistics in the received sequence that contribute to an increase of the magnitude of this spectral line relative to the self-noise power, a fact which might explain the improved MSE performance in the presence of oversampling.

In the case of $P = 4$, from the comparison of the performances of estimators (11) and (12), which estimate $f_e$ by taking into account the information provided by only one spectral line and all the $P$ spectral lines of $\widetilde{C}_{4x}(\alpha; 0)$, respectively, one can observe that both the theoretical and experimental results depicted in Figure 1 show that estimator (12) does not significantly improve the performance of (11), especially in the low SNR range. In fact, the experimental MSE results of (12) are even worse than those of (11) in the low SNR regime. This is due to the fact that the additional harmonics that are exploited in (12) have small magnitudes and their location information can be easily corrupted by the additive noise. Figure 3 shows the magnitudes of these harmonics versus the cyclic frequency. Thus taking into account all the harmonics appears not to be justifiable from a computational and performance viewpoint.

*Experiment* 2. *Performance with respect to timing error* $\epsilon$

In Figure 2, the theoretical and experimental MSEs of FO estimator (11) are plotted versus the timing error $\epsilon$, assuming the following parameters: SNR = 15 dB, and two oversampling factors $P = 1$ and $P = 4$. It turns out once again that oversampling of the received signal helps to improve the performance of symbol-spaced estimators and a significant improvement is achieved (several orders of magnitude) in the presence of large timing offsets ($\epsilon \approx 0.5$). Moreover, the oversampling-based FO estimator is quite robust against the timing errors.

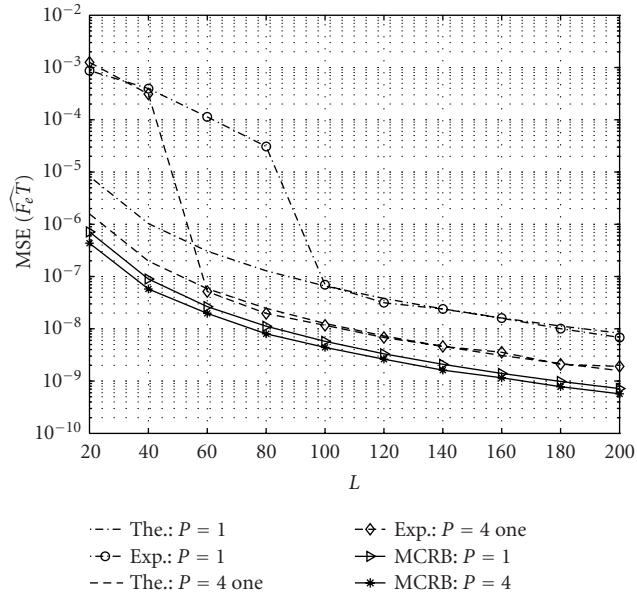


Figure 4: MSEs of $\widehat{F_eT}$ versus number of symbols ($L$).

*Experiment* 3. *Performance with respect to the number of input symbols* $L$

In Figure 4, the theoretical and experimental MSEs of FO estimator (11) are plotted versus the number of input symbols $L$, assuming SNR = 15 dB and timing delay $\epsilon = 0.3$. It can be seen that when the number of input symbols $L$ increases, the experimental MSE results are well predicted by the theoretical bounds derived in Section 4. This plot also shows the potential of these estimators for fast synchronization of burst transmissions since the proposed frequency estimator with $P > 1$ provides very good frequency estimates even when a reduced number of symbols are used ($L = 60 \div 80$ symbols). From Figures 1 and 4, one can distinguish at least two beneficial effects of oversampling: (1) a better MSE performance at medium and high SNRs, and (2) a lower threshold effect (a reduced SNR or number of samples) under which the estimated (simulated) MSE performance of carrier estimators exhibits a sudden increase and departure from the theoretical (analytical) MSE expression. In other words, oversampling proves useful in reducing the outlier effects.

*Experiment* 4. *Performance with respect to the oversampling factor* $P$

In this experiment, we study more thoroughly the effect of the oversampling rate $P$ on FO estimators. By fixing SNR = 15 dB, $\epsilon = 0.3$, and varying the oversampling rate $P$, we compare the experimental MSEs of estimator (11) with its theoretical variance. The result is depicted in Figure 5. It turns out that increasing $P$ does not improve the performance of the FO estimator as long as $P \geq 2$ does. This invariance result is a pleasing property since large sampling rates result in higher implementation complexity and hardware cost, which are not desirable for high-rate transmissions. We remark that a rigorous proof of this invariance result might be

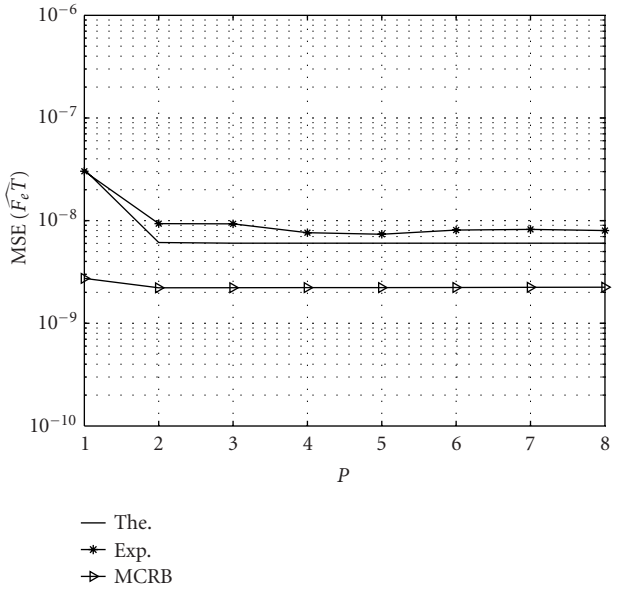


FIGURE 5: MSEs of $\widehat{F_eT}$ versus oversampling factor $P$.

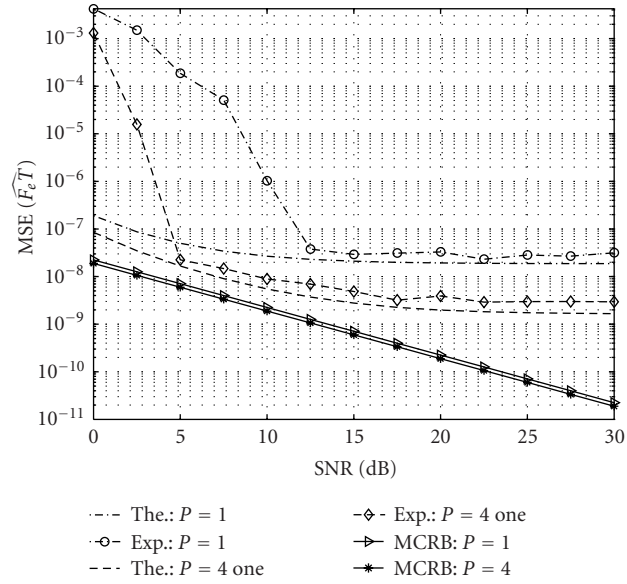


FIGURE 6: MSEs of $\widehat{F_eT}$ versus SNR in frequency-selective channels.

obtained by extending the results from [9, 21], where a similar invariance property has been established in the context of the second-order CS-statistics-based carrier frequency estimators. However, such a proof appears to be extremely difficult and lengthy in the case of the present estimation set-up due to the higher-order statistics involved, and for this reason, it is deferred to a future investigation.

### *Experiment* 5. *Performance with respect to SNR in frequency-selective channels*

Figure 6 shows the results when FO estimator (11) is applied assuming a two-ray frequency-selective channel. Assuming the baseband channel impulse response $h_c^{(\mathrm{ch})}(t) = 1.4\delta(t - 0.2T) + 0.6\delta(t - 0.5T)$, we compare the experimental MSEs with the theoretical asymptotic variances for estimator (11) in two scenarios. $P = 1$ and $P = 4$, respectively. Figure 6 shows again the merit of the FO estimator with $P > 1$.

### *Experiment* 6. *Performance with respect to SNR in time-varying fading channels for* 16-*QAM*

For the sake of completeness, we illustrate, in Figure 7, the numerical results for 16-QAM constellation. The influence of the time-varying fading process is also examined. The number of symbols is $L = 512$, and we assume a Rician fading process with normalized energy and Rician factor $K = 5$. The Doppler spread $f_d$ is chosen as 0, 0.005, and 0.05, respectively, and the Rayleigh fading component is created by passing a unit-power zero-mean white Gaussian noise process through a normalized discrete-time filter, obtained by bilinearly transforming a third-order continuous-time all-pole filter, whose poles are the roots of the equation $(s^2 + 0.35\omega_d s + \omega_d^2)(s + \omega_d) = 0$, where $\omega_d = 2\pi f_d/1.2$. It can be seen that the performance of the proposed estimators deteriorates with $f_d$ increasing, and it exhibits an error floor due to the large self-induced noise caused by the higher-order QAM

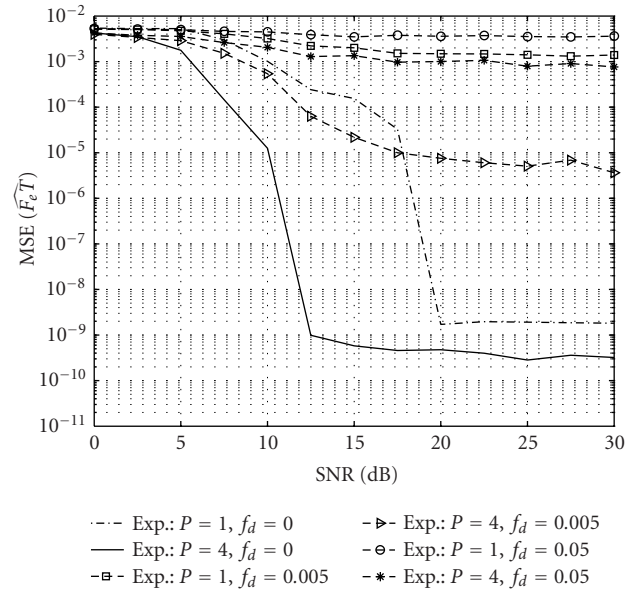


FIGURE 7: MSEs of $\widehat{F_eT}$ versus SNR in time-varying channels for 16-QAM.

constellations. Once again, the results of Figure 7 corroborate the conclusion that the oversampling process improves the performance of carrier frequency estimators.

## 6. CONCLUSIONS

This paper analyzed the performance of a class of non-data-aided feedforward carrier frequency offset estimators for linearly modulated QAM-signals. It is shown that this class of cyclic frequency offset estimators is asymptotically a family of NLS estimators that can be used for synchronization of signals transmitted through AWGN channels with unknown timing errors. The asymptotic performance of these

estimators is established in closed-form expression and compared with the modified CRB. It is shown that this class of FO estimators exhibits a high convergence rate, and in the presence of ISI effects, its performance can be significantly improved by oversampling the received signal with a small oversampling factor ($P = 2$). This work can also be extended to other types of modulations (M-PSK, MSK), and to flat/frequency-selective fading channels.

## REFERENCES


[1] O. Besson and P. Stoica, "Frequency estimation and detection for sinusoidal signals with arbitrary envelope: a nonlinear least-squares approach," in *Proc. IEEE Int. Conf. Acoustics, Speech, Signal Processing (ICASSP '98)*, vol. 4, pp. 2209–2212, Seattle, Wash, USA, May 1998.

[2] J. C.-I. Chuang and N. R. Sollenberger, "Burst coherent demodulation with combined symbol timing, frequency offset estimation, and diversity selection," *IEEE Trans. Communications*, vol. 39, no. 7, pp. 1157–1164, 1991.

[3] P. Ciblat, P. Loubaton, E. Serpedin, and G. B. Giannakis, "Performance analysis of blind carrier frequency offset estimators for noncircular transmissions through frequency-selective channels," *IEEE Trans. Signal Processing*, vol. 50, no. 1, pp. 130–140, 2002.

[4] M. Ghogho, A. Swami, and A. K. Nandi, "Non-linear least squares estimation for harmonics in multiplicative and additive noise," *Signal Processing*, vol. 78, no. 1, pp. 43–60, 1999.

[5] M. Ghogho, A. Swami, and T. Durrani, "On blind carrier recovery in time-selective fading channels," in *Proc. 33rd Asilomar Conference on Signals, Systems and Computers*, vol. 1, pp. 243–247, Pacific Grove, Calif, USA, 1999.

[6] G. B. Giannakis, "Cyclostationary signal analysis, statistical signal processing," in *Digital Signal Processing Handbook*, V. K. Madisetti and D. Williams, Eds., pp. 17.1–17.28, CRC Press, Boca Raton, Fla, USA, 1998.

[7] F. Gini and G. B. Giannakis, "Frequency offset and symbol timing recovery in flat-fading channels: a cyclostationary approach," *IEEE Trans. Communications*, vol. 46, no. 3, pp. 400–411, 1998.

[8] K. E. Scott and E. B. Olasz, "Simultaneous clock phase and frequency offset estimation," *IEEE Trans. Communications*, vol. 43, no. 7, pp. 2263–2270, 1995.

[9] P. Ciblat, E. Serpedin, and Y. Wang, "On a blind fractionally sampling-based carrier frequency offset estimator for noncircular transmissions," *IEEE Signal Processing Letters*, vol. 10, no. 4, pp. 89–92, 2003.

[10] Z. Ding, "Characteristics of band-limited channels unidentifiable from second-order cyclostationary statistics," *IEEE Signal Processing Letters*, vol. 3, no. 5, pp. 150–152, 1996.

[11] G. Feyh, "Using cyclostationarity for timing synchronization and blind equalization," in *Proc. 28th Asilomar Conference*, vol. 2, pp. 1448–1452, Pacific Grove, Calif, USA, October–November 1994.

[12] F. Mazzenga and F. Vatalaro, "Parameter estimation in CDMA multiuser detection using cyclostationary statistics," *Electronics letters*, vol. 32, no. 3, pp. 179–181, 1996.

[13] J. G. Proakis, *Digital Communications*, McGraw-Hill, New York, NY, USA, 3rd edition, 1995.

[14] D. R. Brillinger, *Time Series: Data Analysis and Theory*, Holden-Day, San Francisco, Calif, USA, 1981.

[15] B. Porat, *Digital Processing of Random Signals: Theory and Methods*, Prentice-Hall, Englewood Cliffs, NJ, USA, 1994.

[16] L. Izzo and A. Napolitano, "Higher-order cyclostationarity properties of sampled time-series," *Signal Processing*, vol. 54, no. 3, pp. 303–307, 1996.

[17] D. R. Brillinger, "The comparison of least-squares and third-order periodogram procedures in the estimation of bifrequency," *Journal of Time Series Analysis*, vol. 1, no. 2, pp. 95–102, 1980.

[18] T. Hasan, "Nonlinear time series regression for a class of amplitude modulated cosinusoids," *Journal of Time Series Analysis*, vol. 3, no. 2, pp. 109–122, 1982.

[19] F. Gini, R. Reggiannini, and U. Mengali, "The modified Cramer-Rao bound in vector parameter estimation," *IEEE Trans. Communications*, vol. 46, no. 1, pp. 52–60, 1998.

[20] S. M. Kay, *Fundamentals of Statistical Signal Processing: Estimation Theory*, Prentice-Hall, Englewood Cliffs, NJ, USA, 1993.

[21] Y. Wang, E. Serpedin, and P. Ciblat, "Blind feedforward cyclostationarity-based timing estimation for linear modulations," *IEEE Transactions on Wireless Communications*, vol. 3, no. 3, pp. 709–715, 2004.


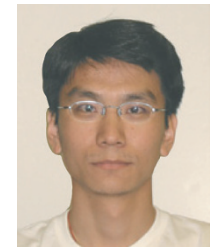

**Y. Wang** received the B.S. degree from Department of Electronics, Peking University, China, in 1996, the M.S. degree from the School of Telecommunications Engineering, Beijing University of Posts and Telecommunications (BUPT), China, in 1999, and the Ph.D. degree from Texas A&M University, College Station, Texas, in December 2003. He is currently an intern with Nokia, Dallas, Texas. His research interests are in the area of signal processing for communications systems.

**K. Shi** received the B.S. degree from Department of Electronic Science and Technology, Nanjing University, China, in 1998, and the M.S. degree from National Communications Research Laboratory, Department of Radio Engineering, Southeast University, China, in 2001. Since January 2002, he has been a Research Assistant with the Department of Electrical Engineering, Wireless Communications Laboratory, Texas A&M University, College Station, Texas, working for his Ph.D. degree. His research interests are in the areas of synchronization and equalization of ultra-wideband systems, OFDM transmissions, PRML channels, and design of turbo/LDPC codes.

**E. Serpedin** received (with highest distinction) the Diploma of Electrical Engineering from the Polytechnic Institute of Bucharest, Bucharest, Romania, in 1991. He received the specialization degree in signal processing and transmission of information from Ecole Superiéure D'Electricité, Paris, France, in 1992, the M.S. degree from Georgia Institute of Technology, Atlanta, Georgia, in 1992, and the Ph.D. degree in electrical engineering from the University of Virginia, Charlottesville, Virginia, in January 1999. From 1993 to 1995, he was an instructor in the Polytechnic Institute of Bucharest, and from January to June 1999, he was a Lecturer at the University of Virginia. In July 1999, he joined Texas A&M University in College Station, Wireless Communications Laboratory, as an Assistant Professor. His research interests lie in the areas of statistical signal processing and wireless communications. He has received the NSF Career Award in 2001, and is currently an Associate Editor for the IEEE Communications Letters and the IEEE Signal Processing Letters.